Characterization of Low-Affinity Complexes between RNA and Small Molecules Using Electrospray Ionization Mass Spectrometry†

Richard H. Griffey,* Kristin A. Sannes-Lowery, Jared J. Drader, Venkatraman Mohan, Eric E. Swayze, and Steven A. Hofstadler

Contribution from Ibis Therapeutics, Isis Pharmaceuticals, 2292 Faraday Avenue, Carlsbad, California 92008

Received May 17, 2000

Abstract: Electrospray ionization mass spectrometry (ESI-MS) provides a sensitive method for the characterization of low-affinity (∼mM) complexes between nucleic acids and small molecules. Such complexes can be generated in solution and moved into the gas phase for detection using MS by reducing the energy imparted during the desolvation process. The affinity and binding stoichiometry of ligands can be determined directly from the observed masses and abundances of the complexes. These benefits are demonstrated for complexes between a 27-mer RNA model of the 16S rRNA, 2-deoxystreptamine (2-DOS), and a series of small organic ligands. We observe two types of 2-DOS−RNA complexes that undergo collisionally activated dissociation in a quadrupole ion trap mass spectrometer at different energies. Molecular modeling results are consistent with this observation. When multiple compounds are mixed with the RNA, the mode of binding can be determined from the abundances of the respective ternary complexes and from the activation energies required to effect gas-phase dissociation in the capillary−skimmer interface region of the instrument. ESI-MS should have considerable utility in studies of macromolecule−ligand complexes where the receptor has multiple binding sites for the ligand.

Introduction

Low-affinity interactions between macromolecules and solution analytes are among the most common in biology and biochemistry. These interactions may be stabilized by one or more contributing forces, such as electrostatic, hydrophobic, or hydrogen-bonding interactions. Examples include binding of anions/cations to proteins and nucleic acids, peptide−peptide complexes, and interactions between receptors and ligands having only partial shape or chemical complementarity. The majority of analytical methods detect formation of such complexes indirectly, as these weak interactions are difficult to observe and characterize. Fluorescence-based methods require labeling of a ligand with a probe molecule, which may alter the binding affinity. Separation-based strategies such as capillary electrophoresis may be used with high concentrations of ligand that drive the binding equilibrium toward the complex. The high concentrations can generate higher order complexes when multiple binding sites exist with similar affinities. Some direct measurement techniques, such as NMR, can be used to observe formation of low-affinity complexes, but determination of binding stoichiometry may be problematic.[1]

Electrospray ionization mass spectrometry (ESI-MS) has been used to characterize noncovalent complexes of small molecules with proteins and nucleic acids.[2,3] ESI-MS-based methods have been employed to accurately measure relative[4−6] and absolute[7,8] solution-phase binding constants, to determine binding stoichiometries of multimeric protein assemblies,[9,10] and to probe the interaction of small molecules with oligonucleotides.[11,12] DNA complexes with groove-binding and intercalating compounds have been studied, establishing both binding stoichiometries and relative affinities.[13,14] Complexes between TAR RNA and small organic molecules and aminoglycosides have been observed using ESI-MS.[15−17] The solution binding affinities and stoichi-

* To whom correspondence should be addressed. E-mail: rgriffey@isisph.com. Phone: (760) 603-2430.

† Abbreviations: ESI-FTICR, electrospray ionization Fourier transform ion cyclotron resonance; CS, capillary skimmer; CAD, collisionally activated dissociation.

(1) Shuker, S. B.; Hajduk, P. J.; Meadows, R. P.; Fesik, S. W. *Science (Washington, D.C.)* **1996**, *274*, 1531−4.
(2) Loo, J. A. *Bioconjugate Chem.* **1995**, *6*, 644−665.
(3) Loo, J. A. *Mass Spectrom. Rev.* **1997**, *16*, 1−23.
(4) Cheng, X.; Chen, R.; Bruce, J. E.; Schwartz, B. L.; Anderson, G. A.; Hofstadler, S. A.; Gale, D. C.; Smith, R. D.; Gao, J.; Sigal, G. B. *J. Am. Chem. Soc.* **1995**, *117*, 8859−60.
(5) Bruce, J. E.; Anderson, G. A.; Chen, R.; Cheng, X.; Gale, D. C.; Hofstadler, S. A.; Schwartz, B. L.; Smith, R. D. *Rapid Commun. Mass Spectrom.* **1995**, *9*, 644−50.
(6) Gao, J.; Cheng, X.; Chen, R.; Sigal, G. B.; J. E., B.; Schwartz, B. L.; Hofstadler, S. A.; Anderson, G. A.; Smith, R. D.; Whitesides, G. M. *J. Med. Chem.* **1996**, *39*, 1949−1955.
(7) Jorgensen, T. J. D.; Roepstorff, P. *Anal. Chem.* **1998**, *70*, 4427−4432.
(8) Sannes-Lowery, K. A.; Griffey, R. H.; Hofstadler, S. A. *Anal. Biochem.* 2000, *280*, 264−271.
(9) Fitzgerald, M. C.; Chernushevich, I. V.; Standing, K. G.; Whitman, C. P.; Kent, S. B. H. *Proc. Natl. Acad. Sci. U.S.A.* **1996**, *93*, 6851−6856.
(10) Schwartz, B. L.; Bruce, J. E.; Anderson, G. A.; Hofstadler, S. A.; Rockwood, A. L.; Smith, R. D.; Chilkoti, A.; Stayton, P. S. *J. Am. Soc. Mass Spectrom.* **1995**, *6*, 459−65.
(11) Loo, J. A.; Thanabal, V.; Mei, H.-Y. *Mass Spectrom. Biol. Med.* 2000, 73−90.
(12) Gale, D. C.; Goodlett, D. R.; Light-Wahl, K. J.; Smith, R. D. *J. Am. Chem. Soc.* **1994**, *116*, 6027−6028.
(13) Wan, K. X.; Shibue, T.; Gross, M. L. *J. Am. Chem. Soc.* 2000, *122*, 300−307.
(14) Gabelica, V.; De Pauw, E.; Rosu, F. *J. Mass Spectrom.* **1999**, *34*, 1328−1337.
(15) Sannes-Lowery, K. A.; Hu, P.; Mack, D. P.; Mei, H.-Y.; Loo, J. A. *Anal. Chem.* **1997**, *69*, 5130−5135.
(16) Mei, H.-Y.; Mack, D. P.; Galan, A. A.; Halim, N. S.; Heldsinger, A.; Loo, J. A.; Moreland, D. W.; Sannes-Lowery, K. A.; Sharmeen, L.; Truong, H. N.; Czarnik, A. W. *Bioorg. Med. Chem. Lett.* **1997**, *5*, 11173-1184.

10.1021/ja0017108 CCC: $19.00
Published on Web 09/30/2000

ometries for ligands and RNA measured using ESI-MS correlate strongly with values determined using other methods.[8] ESI-MS now is an established method for the study of noncovalent complexes involving nucleic acids.[18−20]

An early ESI-MS study by Loo and associates demonstrated that binding interactions between low-affinity peptides also could be observed using ESI-MS.[21] While the binding affinity of the complexes was relatively weak (e.g., ∼mM), they could still be detected via ESI-MS. In other work, the binding of a pyrazine derivative to calmodulin ($K_D \approx 800\ \mu$M) was detected in the presence of Ca^{2+} ions.[22] Similar low-affinity complexes with nucleic acids have not been reported, but anecdotal evidence has suggested that low-affinity complexes of nucleic acids may be detected under appropriate conditions. Muddiman and co-workers observed complexes of piperidine with an oligonucleotide when the temperature of the desolvation capillary was reduced.[23] However, ESI-MS detection of complexes between low-affinity ligands and nucleic acids has not been exploited to date.

We have studied the interactions of 2-deoxystreptamine and five organic compounds with a 27-nucleotide RNA model of the 16S rRNA A-site (16S).[19,24] A critical feature of these experiments is the reduction in the "harshness" of the ESI process realized by adjusting the capillary−skimmer potential difference and employing low desolvation capillary temperatures. These conditions desolvate the ions formed during the electrospray process while minimizing the displacement of low-affinity ligands. 16S−ligand complexes have been observed for neutral and positively charged compounds with low affinities. The binding stoichiometry can be determined from direct observation of ternary or quaternary complexes between 16S and multiple ligands. In a case where one ligand binds at two sites, we demonstrate the nonequivalence of the sites using collisionally activated dissociation (CAD) MS/MS. We also show that ESI-MS uniquely characterizes ternary complexes of RNA and two ligands that bind concurrently through measurement of the gas-phase activation energy for dissociation.[25,26] ESI-MS of low-affinity ligands should have utility in the discovery of novel chemical motifs that bind to nucleic acids and are not detected using other analytical techniques. These methods should be broadly applicable for study of other classes of ligand−receptor interactions.

Materials and Methods

Compounds. 2′-*O*-ACE-protected 27-mer RNA (GGCGUCACAC-CUUCGGGUGAAGUCGCC) was purchased from Dharmacon Research (Boulder, CO). Aqueous solutions were deprotected for 30 min at 60 °C in a 0.1 M tetramethylenediamine acetate buffer at pH 3.5. The resulting solution was evaporated to dryness under reduced pressure, and a stock RNA solution (80 μM) was prepared in 50 mM ammonium acetate buffer, pH 7.0. All chemicals were purchased from Aldrich Chemicals (Milwaukee), except for 2-deoxystreptamine and 3,5-diamino-1-*N*-methyltriazole, which were prepared according to literature methods.[27,28] Ligands were added to the indicated final concentrations from 20 mM aqueous solutions. Final RNA concentrations of 5 μM were prepared by dilution with 50 mM ammonium acetate buffer, pH 7.0, and 30% isopropyl alcohol was added to assist the desolvation process.

ESI-MS. Mass spectrometry experiments have been performed with an LCQ quadrupole ion trap mass spectrometer (ThermoQuest, San Jose, CA) and with a 7.0 T Apex IIe Fourier transform ion cyclotron resonance (FTICR) mass spectrometer (Bruker, Billerica, MA) operating in the negative ionization mode. For the LCQ mass spectrometer, the electrospray needle voltage was adjusted to −3.5 kV, and the spray was stabilized with a sheath gas pressure of 50 psi and an auxiliary gas pressure of 20 psi (60:40 N_2/O_2). The sample was introduced at 2.5 μL/min. The capillary interface was heated to a temperature of 180 °C. The He gas pressure in the ion trap was held at 1 mTorr (uncorrected). MS/MS experiments on the LCQ employed a 1.5 Da isolation window having the desired *m*/*z*. Ions were selected via resonance ejection and stored with $q = 0.2$. The excitation rf voltage was applied to the end caps for 30 ms and increased stepwise over the specified range (0.2−1.6 V_{pp}). A total of 64 scans comprised of 8 microscans were summed over *m*/*z* 1600−2000 following ion trapping for ∼200 ms.

Identical sample preparations were used for experiments with the FTICR mass spectrometer. The electrospray needle voltage was adjusted to −4.0 kV, and the spray was stabilized with a gas pressure of 45 psi (50:50 N_2/O_2). The sample was introduced at 1.0 μL/min. The capillary interface was unheated. Ions were accumulated for 1.25 s in a hexapole ion guide prior to transfer to the trapped ion cell. The indicated gas pressure over the vacuum pump situated below the hexapole ion guide was $\sim 8 \times 10^{-6}$ mbar. The parallel measurements of relative activation energy for ammonia-adducted ions and all small-molecule complexes were performed with the FTICR mass spectrometer by varying the potential difference between the capillary exit and the skimmer cone. For capillary−skimmer (CS) CAD with the FTICR mass spectrometer, CS voltage differences of −115, −125, −135, −145, −155, −175, −195, and −215 V were used to generate the data. Ammonia adducts were observed for all RNA-containing species at the three lowest CS potential differences (see Figure 1). The abundances of free and ammonia-adducted small-molecule−RNA complexes were summed in all cases. Typically, 32 1.2 s transients of 512K data points were summed prior to Fourier transformation and display. No mass-selective MS/MS experiments were performed using the FTICR instrument. Relative solution binding affinities for ligands were determined by measuring the intensities of the 16S−ligand complexes at a 100 μM ligand concentration, normalized to the intensity of the signal from free 16S.

Molecular Modeling. We have used the QXP software to determine the optimal geometry of the ligand−target RNA complex.[29] In the current work, the RNA is held fixed whereas the ligand is treated as completely flexible. The QXP method employs a Monte Carlo perturbation method in conjunction with energy minimization to explore the conformational space in a robust manner. QXP uses a modified version of the AMBER force field with a distance-dependent dielectric of $4.0r$.[30] The formal charges on the phosphate oxygen atoms have been scaled down by 80% to account for the absence of explicit solvent molecules or counterions in the calculations. During the search process, a random translational movement between 0.5 and 15 Å was given to the ligand.

We have used the solution structure of the gentamycin−16S RNA as determined by NMR in our docking calculations (PDB entry 1BYJ).

(17) Mei, H. Y.; Cui, M.; Heldsinger, A.; Lemrow, S. M.; Loo, J. A.; Sannes-Lowery, K. A.; Sharmeen, L.; Czarnik, A. W. *Biochemistry* **1998**, *37*, 14204−12.

(18) Hofstadler, S. A.; Griffey, R. H. *Chem. Rev., in press*.

(19) Griffey, R. H.; Hofstadler, S. A.; Sannes-Lowery, K. A.; Ecker, D. J.; Crooke, S. T. *Proc. Natl. Acad. Sci. U.S.A.* **1999**, *96*, 10129−10133.

(20) Hofstadler, S. A.; Sannes-Lowery, K. A.; Crooke, S. T.; Ecker, D. J.; Sasmor, H.; Manalili, S.; Griffey, R. H. *Anal. Chem.* **1999**, *71*, 3436−3440.

(21) Loo, J. A.; Holsworth, D. D.; Root-Bernstein, R. S. *Biol. Mass Spectrom.* **1994**, *23*, 6−12.

(22) Lafitte, D.; Benezech, V.; Bompart, J.; Laurent, F.; Bonnet, P. A.; Chapat, J. P.; Grassy, G.; Calas, B. *J. Mass Spectrom.* **1997**, *32*, 87−93.

(23) Muddiman, D. C.; Cheng, X. H.; Udseth, H. R.; Smith, R. D. *J. Am. Soc. Mass Spectrom.* **1996**, *7*, 697−706.

(24) Fourmy, D.; Recht, M. I.; Blanchard, S. C.; Puglisi, J. D. *Science (Washington, D.C.)* **1996**, *274*, 1367−1371.

(25) Li, Y.-T.; Hsieh, Y.-L.; Henion, J. D.; Ocain, T.; Ganem, B. *J. Am. Chem. Soc.* **1994**, *116*, 7487−7493.

(26) Gao, J.; Wu, Q.; Carbeck, J.; Lei, Q. P.; Smith, R. D.; Whitesides, G. M. *Biophys. J.* **1999**, *76*, 3253−3260.

(27) Georgiadis, M. P.; Constantinou-Kokotou, V.; Kokotos, G. *J. Carbohydr. Chem.* **1991**, *10*, 739−748.

(28) Kaiser, D. W.; Roemer, J. J. *US Patent 2,648*,670, 1953.

(29) McMartin, C.; Bohacek, R. S. *Comput.-Aided Mol. Des.* **1997**, *11*, 333.

(30) Weiner, S. J.; Kollman, P. A.; Case, D. A.; Singh, U. C.; Ghio, C.; G, A.; Profeta, S.; Weiner, P. *J. Am. Chem. Soc.* **1984**, *106*, 765.

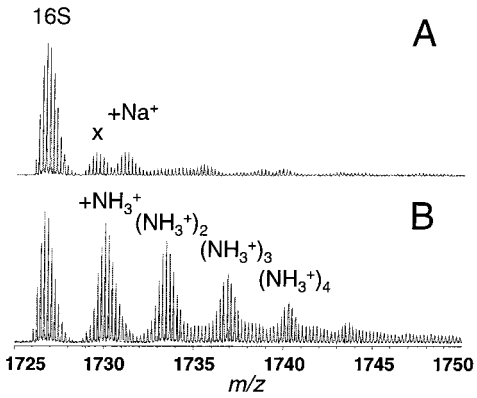

Figure 1. Observation of ammonia-adducted ions of 16S as a function of desolvation conditions. (A) No ammonia-adducted ions observed at a −165 V capillary exit−skimmer potential. The two labeled mass signals arise from a methylated impurity in the RNA (x; M + 14.016 Da) and sodium-adducted species (+Na; M + 21.982 Da represents the mass increase for replacement of a proton by a sodium ion), respectively. (B) At a −115 V capillary exit−skimmer potential, a series of peaks from ammonia-adducted ions are observed at 17.030 Da intervals.

At the start of the calculation, gentamycin was pulled outside the pocket and the torsion angles were randomized. Docking searches using QXP resulted in an rms difference between the lowest energy docked structure and the energy-minimized NMR structure of less than 0.5 Å. We observed a good correlation between the rms deviation and energy of the docked structure.

Results

Detection of weak noncovalent complexes using ESI-MS is a function of both instrument parameters and solution conditions. In solution, high concentrations of buffer can be used to reduce formation of nonspecific electrostatic or hydrogen-bonded aggregates. The observation of weak complexes depends on the level of collisional activation that occurs along the path from the atmospheric region to the high-vacuum region. Variables that impact the degree of collisional activation include the flow rate and temperature of the countercurrent drying gas, desolvation capillary temperature, ESI needle position, CS potential difference, droplet size, and pressure in the region of the supersonic expansion beyond the desolvation capillary. These variables are not independent, and must be iteratively adjusted on any ESI-MS instrument to optimize the detection of weak noncovalent complexes.

We use the abundance of 16S−ammonia ion complexes as a measure of the harshness of the ESI and desolvation processes for RNA targets and their complexes. As shown in Figure 1a, the FTICR source with an unheated desolvation capillary and a −165 V CS potential leads to complete desolvation of 16S with concomitant dissociation of bound ammonium ions to release ammonia. Ions with adducted sodium and potassium cations that are not released during desolvation appear at higher *m*/*z* values. Decreasing the capillary−skimmer potential to −115 V generates the spectrum shown in Figure 1b. The identity of the ammonia-adducted ions could be established unambiguously from accurate measurement of the mass difference ($\Delta(m/z) = 3.406 \pm 0.001$) relative to the $[M - 5H^+]^{5-}$ ions of 16S. Residual waters have been removed, but a series of ammonia-adducted species are observed at *m*/*z* 3.4 intervals. Under these conditions, *noncovalent complexes stabilized by a single hydrogen bond can be observed*. In a similar manner, lowering the desolvation capillary temperature from 180 to 125 °C and increasing the capillary−skimmer potential difference from −25 to −45 V generated ammonia-adducted ions of 16S on the quadrupole ion trap mass spectrometer (with lower resolution).

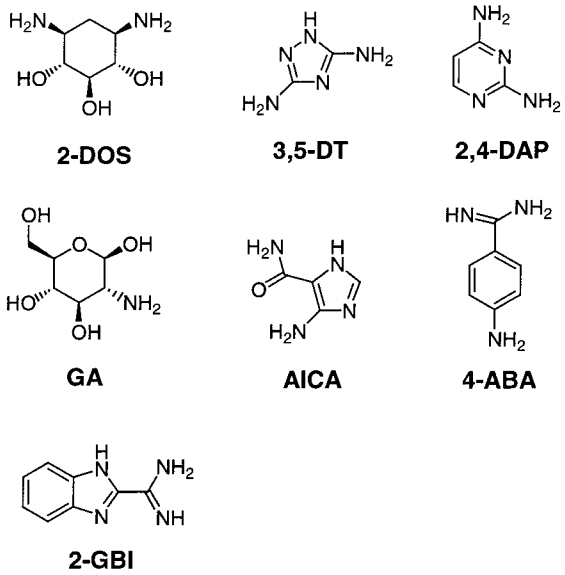

Figure 2. Structures of 16S ligands.

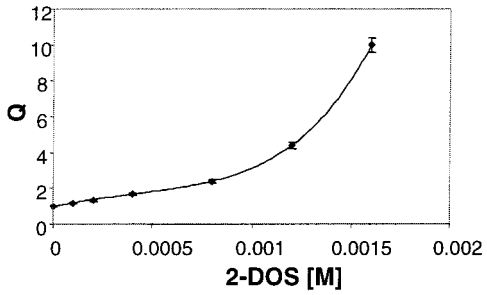

Figure 3. Polynomial fit of Q (the sum of the ion intensities from 16S and all 2-DOS−16S complexes divided by the intensity of 16S) versus 2-DOS concentration (M) in the presence of 50 mM ammonium acetate buffer. The calculated K_D values for 2-DOS, $(2\text{-DOS})_2$, $(2\text{-DOS})_3$, and $(2\text{-DOS})_4$ were 0.6, 1.4, 4, and 15 mM, respectively. All experiments were performed on the LCQ mass spectrometer at a CS potential difference of −125 V under conditions described in the Materials and Methods.

2-Deoxystreptamine (2-DOS; Figure 2) binds to 16S at multiple locations as a function of increasing concentration. Unlike ammonia, 2-DOS dissociation from the 16S complex is not observed at moderate CS potential differences. All 2-DOS binding experiments were performed at a CS potential difference of −165 V. At 0.33 mM, one 2-DOS binds 16S, generating an $[M - 5H^+]^{5-}$ complex observed at *m*/*z* 1758.9. Complexes corresponding to three and four 2-DOS molecules binding concurrently to 16S appear at concentrations above 3.3 mM. Knowledge of the binding stoichiometry leads to the use of a fourth-order polynomial for calculation of the respective dissociation constants (K_D).[31] As shown in Figure 3, the 2-DOS binding data could be fit to a fourth-order polynomial ($R^2 = 0.99$), with estimated K_D values of 0.61 ± 0.08, 1.4 ± 0.1, 4 ± 1, and 15 ± 8 mM.

The nature of the binding of 2-DOS at two distinct sites on 16S has been investigated using CAD and MS/MS on the quadrupole ion trap mass spectrometer. CAD of ions from the 2-DOS−16S complex at *m*/*z* 1758.9 yields ions from unbound 16S. As the relative dissociation energy is increased (Figure 4)

(31) Greig, M. J.; Gaus, H.; Cummins, L. L.; Sasmor, H.; Griffey, R. H. *J. Am. Chem. Soc.* **1995**, *117*, 10765−10766.

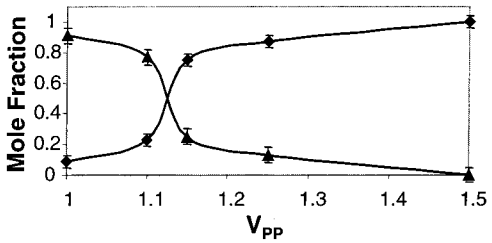

Figure 4. Effective dissociation energy versus the mole fraction of ions observed from undissociated 2-DOS−16S (▲) and free 16S (◆). All experiments were performed on the LCQ mass spectrometer at a CS potential difference of −165 V under conditions described in the Materials and Methods.

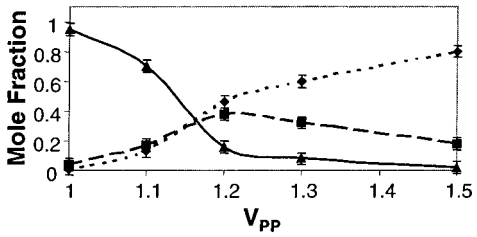

Figure 5. Effective dissociation energy versus the mole fraction of ions observed from undissociated bis(2-DOS)−16S (▲), 2-DOS−16S (■), and 16S (◆), respectively. All experiments were performed on the LCQ mass spectrometer at a CS potential difference of −165 V under conditions described in the Materials and Methods.

the complex is dissociated into free 16S ions and 2-DOS, with 1.13 V yielding 50% dissociation (E_{50}).[26] Next, we have studied the CAD of the bis(2-DOS)−16S complex at *m*/*z* 1791.4. As shown in Figure 5, the E_{50} of the bis(2-DOS)−16S complex was also 1.13 V, but the product ions were composed of both free 16S and the 2-DOS−RNA complex. The abundance of the resulting 2-DOS−16S complex increased as the power was increased to 1.21 V, and then started to decrease at higher activation energies, with free 16S ions as the major product. We investigated the stability of the 2-DOS−16S complex generated from the bis(2-DOS)−16S complex in an MS/MS/MS experiment (data not shown). First, the 2-DOS−16S complex product was isolated following CAD of the bis(2-DOS)−16S complex. These ions were then subjected to additional CAD at different activation energies. The conversion of the 2-DOS−16S complex to free 16S ions was abrupt relative to that in Figure 4, with an E_{50} of 1.17 V. In contrast to the ions which started as a 2-DOS−16S complex, complete dissociation of the 2-DOS−16S ions generated from the bis(2-DOS)−16S complex occurred at 1.3 V.

Potential binding sites for 2-DOS on 16S have been investigated using molecular modeling. Prior work suggested the preferred binding site for 2-DOS on 16S was near the site where the 2-DOS ring binds as part of neomycin-class aminoglycosides.[32] We have used QXP, a Monte Carlo-based conformational search algorithm, to locate the potential binding sties for 2-DOS on the RNA using 200 random initial coordinates. The model in Figure 6 suggests 2-DOS has two high-probability binding sites corresponding to the location of the 2-DOS ring in neomycin-class aminoglycosides (upper right) and at the location of the L-idose ring (lower left) in paromomycin as determined by NMR spectroscopy.[24] Additional higher energy binding sites are observed along the wall of the major groove generated by the bulged A1492 and A1493 residues.

We have used the mass spectrometry assay to identify other ligands that bind to 16S with low affinity. The compounds 3,5-diaminotriazole (3,5-DT; Figure 2) and 2,4-diaminopyrimidine (DAP; Figure 2) both bind weakly to 16S. In a subsequent step, we have mixed pairs of ligands with 16S and used ESI-MS to study the stoichiometry of the resulting complexes. A solution containing 5 μM 16S and 100 μM 2-DOS was mixed with 0.5 mM 3,5-DT. ESI-MS produces signals from free 16S, 3,5-DT−16S, and 2-DOS−16S (Figure 7). An additional signal is observed from the ternary complex formed between 16S and the two low-affinity ligands 2-DOS and 3,5-DT at *m*/*z* 1778.5. The formation of this ternary complex is consistent with simultaneous *concurrent* binding of both ligands at different locations on the RNA surface. In addition, a ternary complex is observed at *m*/*z* 1791 produced by concurrent binding of two 2-DOS ligands. Binding of 3,5-diamino-1-*N*-methyltriazole to 16S was not observed at 0.5 mM ligand by ESI-MS. That the addition of a methyl group at N1 is sufficient to preclude binding of the 3,5-DT to 16S suggests a hydrogen bond from N1 is

(32) Leclerc, F.; Karplus, M. *Theor. Chem. Acc.* **1999**, *101*, 131−137.

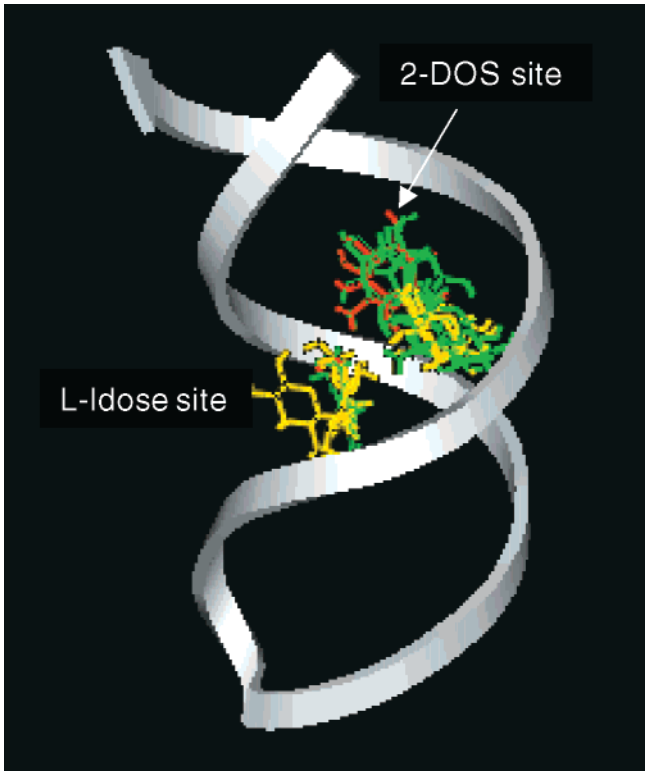

Figure 6. Potential 2-DOS binding sites on the RNA surface located using the QXP modeling program.

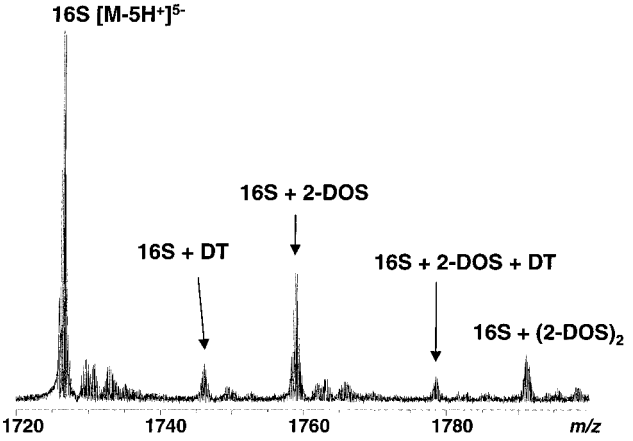

Figure 7. ESI-FTICR MS spectrum from a solution containing 100 μM 2-DOS, 0.5 mM 3,5-DT, and 5 μM 16S. Concurrent binding of 2-DOS and 3,5-DT to 16S is observed for the $[M - 5H^+]^{5-}$ ions.

Table 1. Relative Activation Energies and Solution Affinities for a Series of Ligand−16S Complexes

compound	rel E_A	rel soln affinity
NH_3	1.00[a]	
2,4-diaminopyrimidine	2.16 ± 0.11	0.17 + 0.04
4-aminoimidazolecarboxamide	2.04 ± 0.16	0.26 + 0.04
glucosamine	2.86 ± 0.21	0.86 + 0.03
2-guanylbenzimidazole	2.12 ± 0.09	0.99 + 0.02
4-aminobenzamidine	4.00 ± 0.28	1.00[b]

[a] All activation energies have been normalized to the activation energy for loss of ammonia. [b] All relative solution affinities have been normalized to 4-aminobenzamidine.

required for binding of the 3,5-DT, or binding occurs at a sterically limited site on 16S. In contrast, aminoalkyl-3,5-DT derivatives complex to 16S with affinities similar to that of 3,5-DT (data not shown). While concurrent binding was observed with 2-DOS and 3,5-DT, only signals from 2-DOS−16S complexes are observed when 2,4-diaminopyrimidine and 2-DOS are mixed with 16S. The lack of a signal from the ternary complex suggests that their preferred binding sites overlap and 2-DOS displaces DAP from 16S.

We have investigated the relative gas-phase activation energies (E_A) for dissociation of a series of ligand−16S complexes using the FTICR mass spectrometer. The relative ion abundances for a series of complexes between 16S and ammonia, glucosamine (GA), 4-aminoimidazole-5-carboxamide (AICA), DAP, 4-aminobenzamidine (ABA), and 2-guanidylbenzimidazole (GBI) as well as a series of their ternary complexes have been measured as a function of the voltage difference between the capillary exit and the skimmer cone. In each case, a plot of the natural logarithm of the ion abundance versus the dissociation potential is linear with $R^2 = 0.99 \pm 0.02$. The slopes have been normalized to the E_A for ammonia, and are listed in Table 1. The relative gas-phase E_A values for AICA, DAP, and GBI are 2.04, 2.16, and 2.12, respectively. The E_A values for GA and ABA are 2.86 and 4.00. The order of these values correlates with the relative solution affinities except for GA, whose relative affinity for 16S is lower than that of GBI. The increase in gas-phase stability for the GA−16S complex may result from additional H-bond contacts between hydroxyl groups and 16S.

The relative E_A values for several ternary complexes have also been measured in parallel with CS CAD using the FTICR mass spectrometer. The GBI−ABA−16S complex dissociates with the E_A of the weaker GBI ligand. However, the E_A values for the GA−AICA−16S and GA−DAP−16S complexes are equal to the higher E_A of the GA−16S complex, rather than the lower E_A values of the AICA and DAP complexes. We have investigated the products from gas-phase dissociation of the GA−AICA−16S and GA−GA−16S ternary complexes using the LCQ mass spectrometer. Isolation and CAD of the GA−GA−16S complex yield GA−16S and 16S in a 3:1 ratio at 50% dissociation. Isolation and CAD of the GA−AICA−16S complex yields AICA−16S and 16S in a 1:1 ratio at 50% dissociation. Hence, the higher E_A for the GA−AICA−16S complex is consistent with the observed product ions where GA or GA and AICA have been displaced from 16S. This result suggests that the AICA may lie deeper in the binding pocket than GA, and dissociation from the ternary complex may be blocked. Alternatively, binding of GA may induce a change in the conformation of the RNA that traps the lower affinity ligand.

Discussion

ESI-MS conditions can be adjusted to detect weak ligand−RNA complexes with ~mM affinities. A number of parameters influence the harshness of the ESI source, including the rate of drying produced by the countercurrent gas, the temperature of the desolvation capillary, the gas pressure in the region of supersonic expansion beyond the desolvation capillary, and the effective electric field generated by the potential difference between the desolvation capillary and the first skimmer cone. We have observed that desolvated ions can be formed from partially desolvated droplets that traverse a low-temperature desolvation capillary when the voltage difference between the capillary and the skimmer cone is increased. Although the improved performance with increased energy would seem to be counterintuitive, the viscous drag of ions following supersonic expansion from the capillary may provide a mild method for removal of residual waters of hydration without disruption of complexes (such as ammonia) stabilized by only a single hydrogen bond.

ESI-MS has many benefits for characterization of such low-affinity noncovalent complexes. The exact molecular mass of each ligand and target can be used as an intrinsic label, obviating the need for fluorescent labeling or radiolabeling of either assay constituent. ESI-MS has demonstrated utility for the real-time determination of kinetic parameters for noncovalent complex formation including binding stoichiometry and absolute affinities.[8] Noncovalent complexes with K_D values ranging from nM to >1 mM can be studied with ESI-MS using the mild desolvation conditions described in this work. ESI-MS analysis of ligand affinities can provide additional information through variation of solution conditions including buffer concentration, pH, and metal ions, or addition of ligands that may compete with the ligand of interest for a binding site.

The initial 2-DOS−16S complex observed at low ligand concentrations may be comprised of an ensemble of binding sites between the ligand and the RNA. CAD of the bis(2-DOS) complex formed at higher 2-DOS concentrations yields a subpopulation of 2-DOS−16S ions that have a higher E_{50} than the initial 2-DOS−16S complex. This is consistent with the initial complex containing a mixture of binding sites that dissociate at different activation energies. This observation of two classes of 2-DOS binding sites using ESI-MS correlates with molecular modeling results that show 2-DOS may have two preferred binding locations. These sites correspond to the positions of the 2-DOS ring and the L-idose ring, respectively, in neomycin-class aminoglycosides. While the exact binding location for low-affinity ligands cannot be established with CS CAD, Monte Carlo-based molecular modeling techniques are well-suited to locate potential binding sites once the identity of the ligand has been established.[32] These models assume a static RNA structure, and have limited utility if ligand binding produces a significant conformational change.

Formation of ternary complexes between two ligands and the RNA target can be observed directly using ESI-MS.[33] When two ligands compete for the same binding location, addition of one ligand leads to a decrease in the intensity of the signal from the complex formed between the RNA and the second ligand. A ternary complex can be formed when the two ligands bind at disparate sites on the RNA. As observed for 2-DOS (Figure 7) multiple binding sites may exist for each ligand, and the MS signal from the ternary complex may originate from an ensemble of binding modes. It is possible to measure the relative gas-phase binding energies of ligands through CAD of the ternary complexes, individually or in parallel. This information can be used to establish the order and proximity of binding when a

(33) Lowery, K.; Mei, H.-Y.; Loo, J. A. *Int. J. Mass Spectrom.* **1999**, *193*, 115−122.

ligand with higher binding energy is preferentially dissociated from the complex. The hydroxyl groups of GA may not compete effectively with waters of hydration for binding to the RNA in solution. However, in the gas phase, these hydroxyls can bind to the desolvated RNA and enhance the stability of the complex compared to that in the solution phase.

The solution dissociation constants and the gas-phase activation energies for dissociation have been correlated for protein−ligand complexes. Li and co-workers demonstrated that the gas-phase dissociation energies and solution dissociation constants for FKBP and a series of inhibitors were correlated.[25] Gao and co-workers studied the gas-phase stability of noncovalent complexes between carbonic anhydrase and a series of sulfonamide inhibitors.[26] They observed that noncovalent complexes with two bound inhibitors could be observed, but that the second inhibitor could be dissociated at lower activation energies. The apo-CA complex with a sulfonamide also was dissociated more easily. Finally, they measured differences in activation energy for complexes between a *p*-NO_2 sulfonamide and the *o*-NO_2 analogue. They proposed that the structures of the gas-phase complexes were similar to the structures of solution complexes. A similar trend has been observed for RNA−ligand complexes, although differences in gas-phase and relative solution affinities are observed that may reflect differences in the nature of ligand binding to RNA.

The fusion of simple chemical moieties onto the ligand can alter the relative solution and gas-phase binding affinities for the RNA target dramatically. Hence, ESI-MS analysis of changes in binding affinity for a series of ligands with different substitutions of methyl, ethyl, phenyl, etc. groups could provide a molecular "ruler" to determine contacts and distances to the RNA, and should provide information on potential sites of acceptable substitution on the ligand. For ligands that bind concurrently, observation of changes in the binding affinity for one ligand as a function of structural variation of the second ligand may be used to define the size of a linker group required to fuse the two ligands into a higher affinity unit. The ability to systematically study the interactions between an RNA construct and one or more RNA-binding ligands has significant implications in the discovery of therapeutic agents, as changes in binding affinity resulting from subtle chemical modifications can be rapidly and reliably evaluated.

Conclusions

Monitoring the binding of low-affinity ligands to RNA targets using ESI-MS offers many advantages. The identities, binding affinities, and stoichiometries of bound ligands can be determined directly from mixtures of compounds in a high-throughput format.[34] In addition, the competitive/concurrent interaction among the RNA and pairs of ligands can be established directly through titration or via measurement of relative activation energies for gas-phase ligand dissociation. The speed of the ESI-MS experiment allows rapid exploration of chemical derivatives of ligands to establish points of contact between the RNA and ligand, and between two ligands bound concurrently to the RNA. The resulting binding can then provide a knowledge base for the design of higher affinity ligands to the target RNA. These techniques should be applicable to other systems such as DNA duplexes and protein−ligand and protein−peptide interactions and will have particular utility when the ligand has multiple binding modes with the target.

Acknowledgment. This work was funded in part through DARPA Grant N65236-99-1-5419. The FTICR mass spectrometer was purchased in part through NIST Grant 97-01-0135.

JA0017108

(34) Sannes-Lowery, K. A.; Drader, J. J.; Griffey, R. H.; Hofstadler, S. A. *Trends Anal. Chem.* **2000**, *19*, 281−291.